Integrating susceptibility maps of multiple hazards and building exposure distribution: A case study of wildfires and floods for Quang Nam province, Vietnam

Chinh Luu[1*], Giuseppe Forino[2], Lynda Yorke[3], Hang Ha[4], Quynh Duy Bui[4], Hanh Hong Tran[5], Dinh Quoc Nguyen[6], Hieu Cong Duong[7], Matthieu Kervyn[8]

[1]Faculty of Hydraulic Engineering, Hanoi University of Civil Engineering, Hanoi, 100000, Vietnam
[2]School of Science, Engineering & Environment, University of Salford, Manchester, M5 4WT, UK
[3]School of Environmental and Natural Sciences, Bangor University, Bangor, Gwynedd, LL57 2DG, UK
[4]Department of Geodesy, Hanoi University of Civil Engineering, Hanoi, 100000, Vietnam
[5]Faculty of Geomatics and Land Administration, Hanoi University of Mining and Geology, Hanoi, 100000, Vietnam
[6]Phenikaa University, Hanoi, 100000, Vietnam
[7]Hanoi University of Civil Engineering, Hanoi, 100000, Vietnam
[8]Department of Geography, Vrije Universiteit Brussel, Brussels, 1050, Belgium

Correspondence to: Chinh Luu (chinhltd@huce.edu.vn)

Abstract. Natural hazards have serious impacts worldwide on society, economy, and environment. In Vietnam, throughout the years, natural hazards have caused significant loss of lives as well as severe devastation to houses, crops, and transportation. This research presents a new approach for multi-hazard (floods and wildfires) exposure estimates using machine learning models, Google Earth Engine, and spatial analysis tools for a typical case study, Quang Nam province in Central Vietnam. A geospatial database is built for multiple hazard modeling, including an inventory of climate-related hazards (floods and wildfires), topography, geology, hydrology, climate features (temperature, rainfall, wind), land use, and building data for exposure assessment. The susceptibility of each hazard is first modeled and then integrated into a multi-hazard exposure matrix to demonstrate a hazard profiling approach for multi-hazard risk assessment. The results are explicitly illustrated for floods and wildfire hazards and the exposure of buildings. Susceptibility models using the random forest approach provide model accuracy of AUC = 0.882 and 0.884 for floods and wildfires, respectively. The flood and wildfire hazards are combined within a semi-quantitative matrix to assess the building exposure to different hazards. Digital multi-hazard exposure maps of floods and wildfires aid the identification of areas exposed to climate-related hazards and the potential impacts of hazards. This approach can be used to inform communities and regulatory authorities on where to develop and implement long-term adaptation solutions.

1 Introduction

Different geographic areas worldwide, including mountainous, delta, and coastal regions, are facing distinct hazards and combinations of hazards (Rentschler et al., 2022). These challenges are intensified by population growth, urbanization,

globalization, and climate change-induced shifts in extreme weather patterns, amplifying their adverse effects (Khatakho et al., 2021; Bangalore et al., 2018). While floods and storms represent the main hazards affecting Asian countries, risks from other hazards, such as landslides and wildfires, are also exacerbated by more extreme climate patterns, land-use changes, and population expansion in these nations (Ipcc, 2022). People who depend on natural resources lose their livelihoods and become more vulnerable (Balica et al., 2015).

Due to its geographical location and unique natural conditions, Vietnam is exposed to various natural hazards: floods, landslides, droughts, and wildfires, further exacerbated by human activities combined with extreme weather conditions (Gan et al., 2021). The central region of Vietnam, particularly Quang Nam province, is highly vulnerable to natural hazards, making sustainable development tasks very challenging (Nguyen et al., 2023). Floods associated with tropical storms during the monsoon season (Luu et al., 2021) and wildfires exacerbated by dry seasons and high temperatures pose frequent threats and require comprehensive assessments of multi-hazard susceptibility and exposure in Quang Nam province (Du et al., 2018). The impacts of these natural hazards hinder local development initiatives and exacerbate socio-economic disparities (Khan et al., 2020). Disrupted agricultural activities, damaged infrastructure, and compromised access to essential services hinder the region's progress, while the loss of lives and properties deepens the social and economic burdens (Skilodimou et al., 2019). Notwithstanding these longstanding issues with floods and wildfires in the Quang Nam province of Vietnam, limited studies have focused on multi-hazard susceptibility and exposure assessments.

Quang Nam province is characterized by a coastal region with low-lying topography facing high flood risks due to heavy rainfall, typhoons, and potential breaches of dams and levees (Chau et al., 2014). The province has two large river catchments: the Vu Gia - Thu Bon and Tam Ky rivers. Away from the coast, the province is characterized by steep, hilly terrains and a dense river network. The prolonged heavy rainfall of the monsoon season in this dissected landscape results in yearly riverine floods in the lowland area and along the coast. This issue holds particular significance for the Quang Nam province because flood events pose a direct threat to human lives and cause significant damage to its infrastructure, education, economic development, and health-related services (Lee et al., 2020).

Wildfires are also a natural hazard with devastating consequences, posing a severe threat to the environment and human communities (Tedim et al., 2015). Wildfires often occur due to a complex interplay of dry weather conditions, high temperatures, low humidity, flammable vegetation, and other geo-environmental factors (Kalantar et al., 2020). Vietnam is particularly prone to fire events, especially in the northern part (Trang et al., 2022) and the Central region (Nguyen et al., 2023). According to the statistical data from the Global Forest Watch, Vietnam has had a total of 674,612 wildfire alerts since 2012 and ranked sixth in Southeast Asia regarding wildfires in the last two decades (Ansori, 2021).

The term "multi-hazard" refers to the fact that hazards often interact in complex ways, and their combined impact might be greater than the sum of individual hazards (Wing et al., 2018). The dynamic interplay between flood probability in wet seasons and wildfire likelihood in dry seasons can be influenced by various factors, including environmental conditions, climatic patterns, topography, vegetation cover, and land use patterns (Skilodimou et al., 2021; Bountzouklis et al., 2022). Wildfires can significantly impact landscape hydrology by destroying vegetation cover and disrupting soil structure,

reducing infiltration rates and heightening surface runoff during subsequent rain events (Mueller et al., 2018). Floods can reduce the formation and expansion of wildfire risks by wetting vegetation and soil, temporarily mitigating the likelihood of ignition and fire spread (Papaioannou et al., 2023). However, flood events can disrupt natural drainage patterns, saturate soils, and promote vegetation development, fueling wildfires in dry seasons (Eisenbies et al., 2007). In general, the formation
70 of multi-hazard events often results from dynamic spatial and temporal interactions among various factors (De Angeli et al., 2022); significantly, floods and wildfires can exacerbate or mitigate each other's impacts depending on seasonal fluctuations, environmental conditions, or extreme climatic variability (Yu et al., 2023). Broadening the assessment framework for these spatial and dynamic interactions can lead to a more comprehensive and accurate risk evaluation (De Angeli et al., 2022). Thus, multi-hazard susceptibility and exposure assessments are required for efficient disaster risk management (Zhou et al.,
75 2015). Multi-hazard susceptibility assessment provides insights into the spatial co-occurrence of different hazard types (Rusk et al., 2022). Multi-hazard exposure assessment enables the evaluation of the potential impact of multi-hazards on people, buildings, and critical facilities, which supports disaster management activities (De Angeli et al., 2022).

Advanced technologies, such as Machine Learning (ML), remote sensing, and big data analytics, play a critical role in predicting, monitoring, and mitigating the impact of hazards (Velev and Zlateva, 2023). Currently, Google Earth Engine
80 (GEE), a cloud-based geospatial processing platform developed by Google in 2010, offers an extensive and up-to-date archive of satellite imagery, robust analysis tools, custom ML algorithm development, and the capacity to integrate multiple data sources (Tamiminia et al., 2020).

Various studies have applied ML algorithms, including Classification And Regression Tree (CART) and Random Forest (RF), in modeling natural hazard susceptibility and have proven the high performance and accuracy of these models (Chen et
85 al., 2018; Kim et al., 2017). CART and RF have been used to build susceptibility maps for single hazards, e.g., forest fire (Pourtaghi et al., 2016) or landslide (Wu et al., 2022), but also in developing the multi-hazard (forest fires and droughts) susceptibility maps for the Gangwon-do region in Korea (Piao et al., 2022), or constructing the multi-hazard (flood, landslides, forest fire, and earthquake) susceptibility maps in Khuzestan Province, Iran (Pourghasemi et al., 2023). Most of these studies have indicated that ML models perform well in estimating multi-hazard susceptibility but have not mentioned
90 multi-hazard exposure assessment. Meanwhile, multi-hazard exposure assessment can help recognize overlapping exposures and comprehend the intricate relationships between several hazards (Wang et al., 2020).

Therefore, the study aims are (i) to present and apply a methodological approach to assess and map susceptibility of multiple hazards for the Quang Nam province; (ii) to utilize two ML models, CART and RF, that have been implemented on the GEE platform to build the susceptibility maps of flood and wildfire hazards for the Quang Nam province; and (iii) to
95 integrate the hazard-specific susceptibility maps with built environment data to assess the multi-hazard exposure.

2 Study area

Quang Nam province is located in the central region of Vietnam, which has significant economic growth and huge tourism potential. Since the "economic reforms" and opening to foreign investment in 1986, Quang Nam province has seen significant socio-economic transformations, such as the development of industrial zones and tourism. However, this fast
100 development presents several issues for the province in pursuing sustainable development, necessitating optimal use of natural and socio-cultural resources (Chau et al., 2014). Quang Nam had a total population of 1.84 million in 2019, with over 73% of the population residing in the coastal plain, comprising just 25% of the total geographical area. The Kinh ethnic group comprises 92.3% of the population; the remainder consists of many ethnic minorities, including the Co Tu, Xo Dang, M'nong, Co, and Gie Trieng (Quang Nam Statistical Office, 2019). Agriculture, forestry, and fisheries accounted for 56 % of
105 the total labor force, although their contribution to the GDP is only 21.4% (Quang Nam Statistical Office, 2019).

Quang Nam encompasses a large topographic gradient, from a coastal plain to steep mountains, with a total area of 10,438 km² (**Figure 1**). The complex topography due to the Annamite Range leads to strong separation in climate conditions and landscape characteristics. Terrain elevation gradually lowers from West to East, with mountainous areas (slope of 15° or more) concentrated mainly in the West following the Annamite Range and the flood plains running along the coastline. The
110 tropical monsoon climate is characterized by two distinct weather seasons in a year: the dry season from March to August, associated with water shortages, leading to droughts, and the rainy season from September to February, often bringing excess water and leading to floods. Quang Nam has the highest annual rainfall in Vietnam, averaging 2,200 mm to 2,700 mm, with 70% falling during the rainy season (https://quangnam.gov.vn/). The main hazards in Quang Nam province are floods, landslides, droughts, and wildfires (Du et al., 2018). This study focuses on assessing and mapping flood and wildfire hazards
115 in the province.
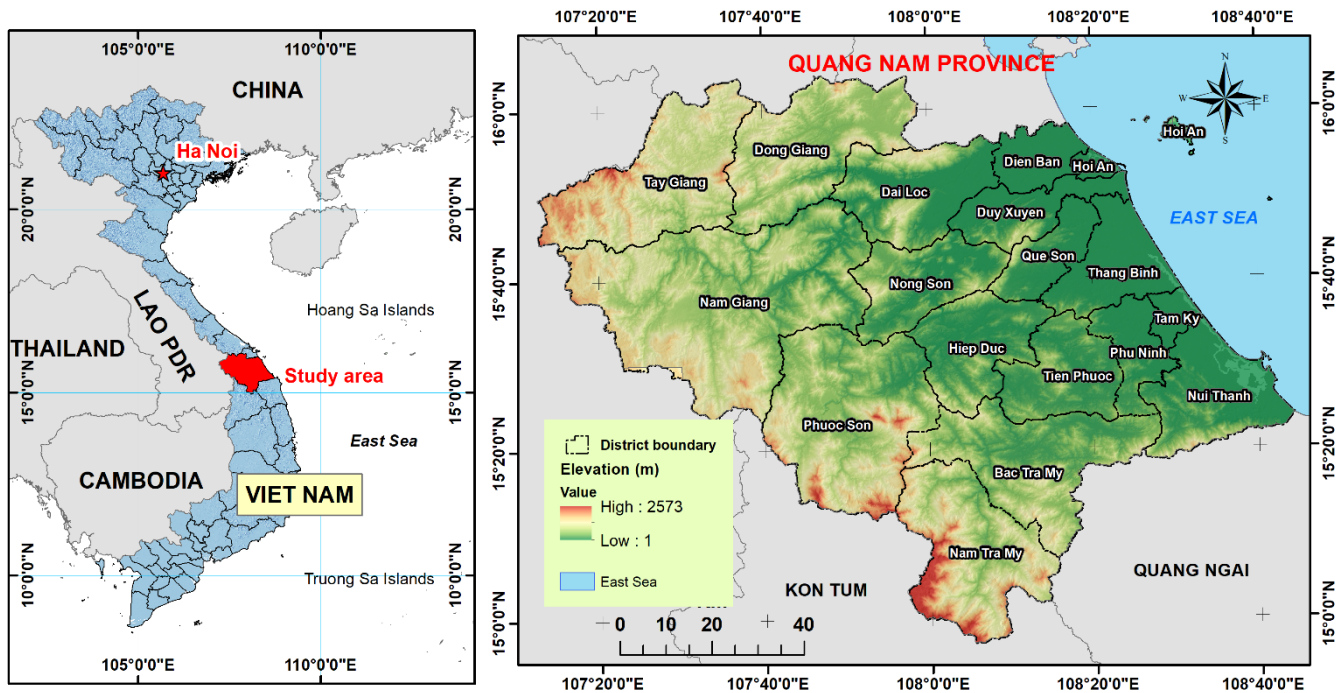
Figure 1. Elevation map of the study area, Quang Nam province in Vietnam (source: Shuttle Radar Topographic Mission Digital Elevation Model)

3 Methodology

3.1 Methodology flowchart

The multi-hazard exposure assessment process comprises seven main stages, as follows: (1) Inventory maps of each hazard were created based on historical data collection; (2) Factors potentially influencing the spatial distribution of floods and wildfire were collected, including topography, geology, hydrology, climate (temperature, wetness, wind), and land use based on their relevance and data availability (Luu et al., 2018; Pham et al., 2021); (3) The influencing factors of each hazard were tested for multicollinearity to enhance the reliability and stability of the model's predictions, (4) CART and RF models were developed on the GEE cloud computing platform to construct susceptibility maps of floods and wildfires separately, (5) The Area Under the ROC Curve (hereafter, AUC) was utilized to assess the predictive performance of the susceptibility maps to choose the best model for each hazard and validate it, (6) The flood susceptibility map and the wildfire susceptibility map were combined to build a susceptibility map for multi-hazard co-occurence, and (7) this multi-hazard susceptibility map was overlaid with the building data to create a multi-hazard exposure map for the study area (**Figure 2**).
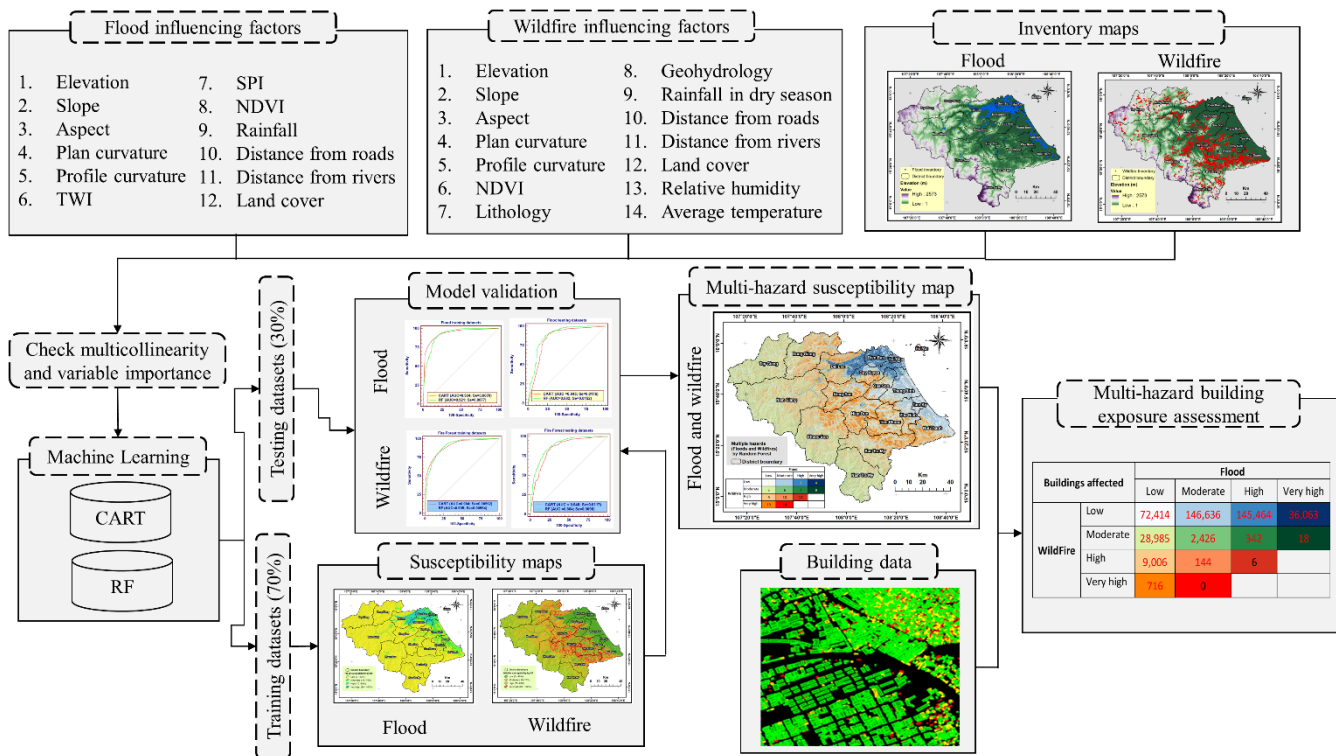
Figure 2. Methodology flowchart for multi-hazard exposure assessment and mapping in this study.

3.2 Data used

3.2.1 Inventories of floods and wildfires

Developing accurate hazard inventories is crucial for susceptibility mapping (Bui et al., 2022). In this study, the flood marker points recorded for all flood events from 2007 to 2023 were considered, as reported by the Quang Nam Provincial Steering Committee of Natural Disaster Prevention and Control. We removed duplicate flood points. A total of 847 historical flood marks were obtained from this database – these correspond mainly to the 2007, 2009, and 2013 flood events with the largest spatial extent. Each flood mark comprises a unique identifier, geographical coordinates (longitude and latitude), flood depth, and provider information. A second source of information was derived from mapping flood extent on SAR data from Sentinel 1 for 2017 to 2023, which we compare with official reports from the Provincial Committee. The flood detection algorithm described in Mai Sy et al. (2023) was implemented in Google Earth Engine. Inundation areas detected on the different Sentinel 1 scenes were overlayed and compared with the flood mark locations to avoid duplicates. 47 new flood sites were detected and integrated as additional points (using the centroid of the flood site), with 847 historical flood marks for the inventory data.

The final flood inventory includes 894 flood locations: 70% of them (626 locations) were randomly selected to calibrate the flood susceptibility model, and the remaining 30% (268 locations) were designated for validating purposes (**Figure 3**). In

addition, 894 non-flood locations were randomly selected across the study area using the "Create random point tool" in ArcGIS software. Non-flood points were chosen only in zones outside the flood-affected zones in our inventory.

150   Additionally, we excluded steep slopes (>10°) or areas of positive relief (such as hilltops) from the selection of non-flood points, as these locations that can not be associated with floods would artificially increase the accuracy of the susceptibility model. The non-flood points were then classified in a ratio of 70/30, mirroring the classification of the flood locations. This process was undertaken to create a comprehensive database for input into the GEE platform, which was utilized for modeling and validation.

155   For the wildfire inventory, this study involved the collection of 1,911 wildfire locations recorded during the dry season (March to August) from 2020 to 2023 (**Figure 3**), from the National Forest Protection Department's website (available at https://watch.pcccr.vn/thongKe/diemChay). This agency utilizes data from many satellites (AQUA, J1, SUOMI, and TERRA) that are regularly received at the TerraScan receiving station located at the National Forest Protection Department. The use of near-infrared bands from many satellites helps to identify the presence of heat associated with active wildfires on

160   the ground (Giglio et al., 2008). The website database was checked and filtered to avoid duplicated wildfire locations, dates, and commune data field conditions. The wildfire location data (points) represent the specific fire sites captured by one type of satellite inside a particular commune at a given time. We filtered the database of the National Forest Protection Department to retain only wildfire spots exceeding a minimum size threshold of 2 hectares, as smaller fire areas should be considered human-induced. To determine the non-fire points, we randomly selected points within the zones with forested

165   and natural vegetation land cover, which were not identified as wildfires in the inventory. We excluded residential areas, water, and crop areas from the selection of non-fire points, as these cannot be associated with wildfires corresponding to the criteria selected in this study and would artificially increase the accuracy of our susceptibility model.
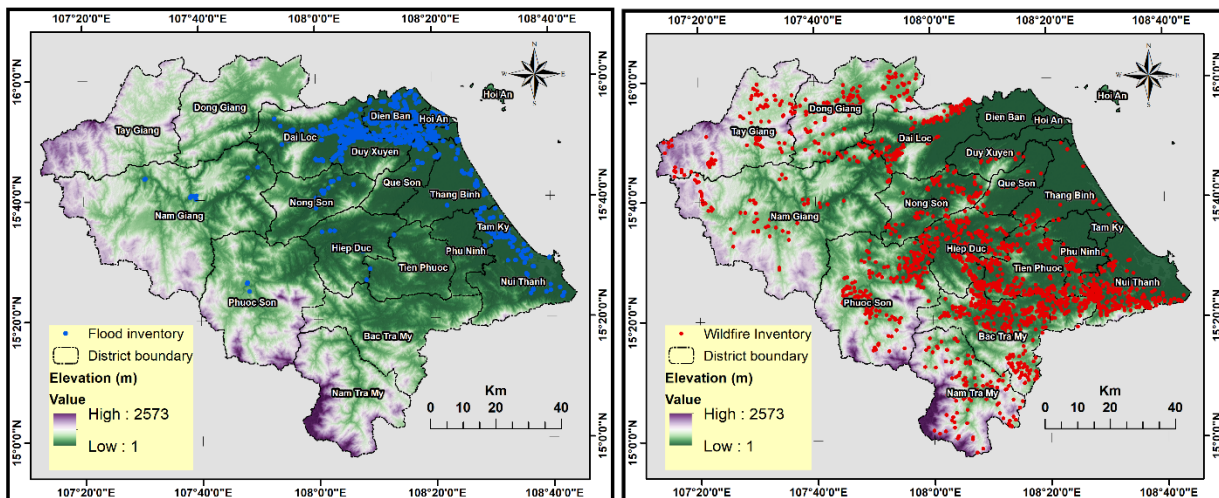
170   **Figure 3. Inventory maps of flood (left) and wildfire (right) points in Quang Nam province.**

3.2.2 Influencing factors

Several factors significantly influence flood and wildfire occurrences. Low-lying areas are prone to flooding, while elevated regions can hinder fires (Pourtaghi et al., 2016; Bui et al., 2022). Slope, slope aspect, and curvature affect water flow, erosion, and fire spread, with steeper slopes either mitigating or accelerating these hazards (Dottori et al., 2018; Trang et al., 2022). The Topographic Wetness Index (TWI) and Stream Power Index (SPI) help quantify water accumulation and erosion risks. Vegetation density, assessed using the Normalized Difference Vegetation Index (NDVI), impacts both flood absorption and fire fuel availability (Abedi Gheshlaghi et al., 2021; Gonzalez-Arqueros et al., 2018). Road and river proximity also influence flood and fire dynamics, while land cover, lithology, and geohydrology influence water retention and fire susceptibility (Ha et al., 2023; Hosseini and Lim, 2022). Rainfall patterns and temperatures, particularly during dry seasons, further contribute to both flood and wildfire risks (Abram et al., 2021; Ahmadlou et al., 2018). These factors are modeled using data from satellite imagery, DEMs, and long-term climate records.

3.2.3 Built environment data

In this study, we use the building data to assess the potential impact of flood and wildfire hazards on building infrastructure, considering housing/building a key livelihood asset. Spatial data on the building infrastructure of Quang Nam province is extracted from the Open Building dataset of Google (https://developers.google.com/earth-engine/datasets/catalog/GOOGLE_Research_open-buildings_v3_polygons). The collection contains information about each building, including a polygon representation of its footprint on the ground and a confidence score showing the level of certainty about its classification as a building (Sirko et al., 2021). We filtered the data with a confidence level of more than 80% and an area larger than 30m for accurate data on buildings (assuming the minimum size for a residential building). The data is created from high-resolution satellite photography with a resolution of 50 centimeters. The selected data was checked visually against Google Earth and was shown to represent the large majority of buildings properly.

This study focuses on buildings in terms of elements exposed to hazards, considering their importance as critical economic assets and reflections of population distribution (Askar et al., 2021). Buildings are essential components of community infrastructure, and damage to them may have big social and economic effects, making them a crucial exposure indicator for risk assessment (Carreño et al., 2007). In addition, buildings often accommodate individuals and vital services; thus, their exposure to hazards and susceptibility to damage directly control the possibility of human fatalities and disturbance to everyday activities. In terms of vulnerability, buildings are not equally at risk from all hazards; their susceptibility varies depending on the hazard type and the structural characteristics of the building, although vulnerability is not considered explicitly in this study (Schneiderbauer and Ehrlich, 2004).

3.3 Methods

3.3.1 Multicollinearity

Variance Inflation Factors (VIF) and Tolerance are critical statistical measures in detecting the presence of multicollinearity among input variables (Arabameri et al., 2018). VIF quantifies how much the variance of an estimated regression coefficient increases due to multicollinearity (Ma et al., 2020). Tolerance is the reciprocal of VIF and reflects the proportion of variance in a predictor that is not forecasted by a combination of other predictors (Bui et al., 2023). Significant multicollinearity among input variables is detected if the VIF value surpasses 10 or the Tolerance value drops below 0.1 (Miao et al., 2023). Variables found to be multicollinear will be deleted from the model, and the model will be run to check for multicollinearity again.

3.3.2 Machine learning approach for hazard susceptibility modeling

This study has developed two ML models, including CART and RF, on the GEE workspace to construct the hazard (flood and wildfire) susceptibility maps for the Quang Nam province.

The CART was first introduced by Breiman et al. (1984). It is an algorithm used for both classification and regression tasks. CART builds binary trees recursively by splitting the dataset into subsets based on the feature values (Tang and Zhang, 2020). Mathematically, this algorithm can be summarised as follows (Ahmadlou et al., 2022):

1. Input a training dataset $D = (Xs, Y)$ where Xs are the feature variable, and Y is the target variable (class labels for classification, numerical values for regression).

2. For the classification issue, the CART algorithm uses the Gini impurity coefficient on these subsets to measure the disorder or impurity of an input dataset. The Gini impurity coefficient is determined using the following equation:

$$Gini(D) = \sum_{i=1}^{J} P_i(1 - P_i) = \sum_{i=1}^{J} P_i - \sum_{i=1}^{J} P_i^2 = 1 - \sum_{i=1}^{J} P_i^2 \qquad (1)$$

where $Gini(D)$ is the Gini impurity coefficient of the input dataset D, J represents the number of classes in the input dataset, and P_i denotes the probability of class i in dataset D.

The CART continues seeking the best feature and threshold recursively until a stopping criterion, such as maximum tree depth (*max_depth*) or minimum samples in a leaf (*min_samples_leaf*). After that, the resulting tree can be used to classify new datasets.

Like all decision tree algorithms, CART is prone to overfitting, especially when the tree becomes too deep. To mitigate this, pruning techniques and hyperparameter tuning are often applied to optimize the tree's structure, ensuring generalizability to unseen data (Ahmadlou et al., 2022).

The RF is a widely used ML algorithm developed by Breiman (2001), which combines the output of multiple decision trees to reach a single result (Naghibi et al., 2016). It is used for both classification and regression tasks (Genuer et al., 2010). The content of this technique can be described as follows (Breiman, 2001):

230   1. Input a training dataset D of N bootstrap samples, $D = (Xs, Y)$ where Xs is the feature variable, and Y is the target variable (class labels for classification, numerical values for regression). The RF technique creates multiple decision trees using bootstrapped subsets of the training data D. Each tree is constructed using N samples drawn with replacement (bootstrap sampling).

       2. For each tree and at each split, a subset of features (m) is randomly selected from the total number of features in the

235 training dataset (M) to ensure diversity among the trees.

       3. Each tree in the RF algorithm is built using the selected bootstrap sample and features in the first and second steps. The tree is developed by recursively dividing the dataset based on the selected features and splitting criteria.

       4. The RF technique combines these predictions (multiple decision trees) due to the specific tasks. The prediction mode from individual trees is the final classification task prediction.

3.3.3 Model validation and comparison

240

This study used the ROC curve and AUC to validate the predictive performance of each hazard susceptibility model, including CART and RF models. The ROC curve is generated by plotting the true positive rate (sensitivity) against the false positive rate (1-specificity) for different threshold values (Carter et al., 2016). Sensitivity quantifies the ability of the model to correctly identify susceptible areas, while specificity measures the capability to identify non-susceptible areas correctly

245 (Meghanadh et al. 2022). The AUC is calculated to quantify the quality of the predictive model. The AUC values vary from 0 to 1, where AUC values of 0.5–0.6 reflect a low predictive performance, 0.7-0.8 is interpreted as a medium predictive performance, 0.8-0.9 indicates good predictive performance, and 0.9-1.0 denotes excellent predictive performance.

3.4 Experimental process

This study employed the GEE cloud computing platform for the pixel-based CART and RF algorithms to build susceptibility

250 maps for flood and wildfire hazards separately. The input data was collected from various sources and formats. First, we pre-processed and converted these data into raster format with 30-meter spatial resolution in a GIS environment. Then, these data were uploaded into the GEE platform. Hyperparameter tuning technique was used to optimize the performance of ML algorithms, as they significantly affect the accuracy, efficiency, and generalization ability of ML models (Schratz et al., 2019). Various hyperparameter tuning methods include grid search, random search, gradient-based optimization, and

255 Bayesian optimization. This hyperparameter tuning process of grid search was used for the modeling in this study, including the following steps:

       1.   Set up the environment: install Python packages in the Google Earth Engine (GEE) Application Programming Interface (API) to handle geospatial data and scikit-learn to develop ML models.

2. Data preparation: upload fifteen landslide-affecting factors to the GEE environment to build the flood and wildfire susceptibility maps. The training and testing datasets have also been uploaded to this platform.

3. Hyperparameter tuning: use scikit-learn to develop various ML models (CART and RF) and define the hyperparameter search spaces for a grid search. This step involves setting reasonable value ranges for each hyperparameter in each model, for CART model (*max_Nodes, minLeafPopulation*) and RF model (*numberOfTrees, variablesPerSplit, bagFraction, seed*), described in **Table 1**. Then, scikit-optimize's grid search performs iterative assessments using the training data to select the hyperparameter combination that optimizes a chosen performance metric (ROC and AUC) on the testing data. The best hyperparameter combinations for each model are determined based on these performance metrics.

4. Model assessment: optionally, the final evaluation involves retraining the predictive models with the chosen hyperparameters on the training data. The performance of these retrained models is then assessed using the ROC curve and AUC value on the validation dataset to gauge their effectiveness.

Table. 1 The hyperparameter values in the optimization process.

Model	Optimized Hyperparameter	Explanation	Lower and upper limits	Optimal value
CART	max_Nodes	The maximum number of leaf nodes in each tree.	2-500	150
	minLeafPopulation	Only create nodes whose training set contains at least this many points.	1-10	2
RF	numberOfTrees	The number of decision trees to create.	100 – 1000	200
	minLeafPopulation	Only create nodes whose training set contains at least this many points.	1-10	1
	bagFraction	The fraction of input to bag per tree.	0.1 – 1.0	0.7
	seed	The randomization seed.	0 - 42	23

4 Results

4.1 Assessment of multicollinearity and variable importance

In this research, the VIF and tolerance values of influencing factors for flood and wildfire susceptibility modeling are
275 satisfactory, so all input factors are selected to develop hazard susceptibility maps (**Table 2**). In natural hazard susceptibility modeling, each input variable may influence the occurrences of each hazard in various ways (Pourghasemi et al., 2020). Variable importance assessment can identify which factors have the most significant impact on the hazard formations (Javidan et al., 2021). RF is one of the most popular ML algorithms for evaluating variable importance by measuring how much they contribute to the model's accuracy (Fox et al., 2017). Thus, this technique was applied to assess the significance
280 of all input variables. The results show that rainfall (weight = 0.1742), distance from rivers (weight = 0.1620), NDVI (weight = 0.1330), and land cover (weight = 0.1159) are the indicators that significantly contribute to the control of the spatial distribution of flood events within the study area.

Table 2 Assessment of multicollinearity and variable importance to flood influencing factors.

Factors	Flood			
	Tolerance	VIF	Variable importance	Rank
Rainfall	0.832	1.225	0.1742	1
Distance from rivers	0.945	1.204	0.1620	2
NDVI	0.759	1.774	0.1330	3
LULC	0.582	2.160	0.1159	4
Aspect	0.98	1.019	0.1095	5
TWI	0.725	1.676	0.0753	6
Distance from roads	0.600	3.241	0.0709	7
Plan Curvature	0.798	3.669	0.0695	8
Profile Curvature	0.876	1.418	0.0320	9
Elevation	0.777	1.259	0.0300	10
Slope	0.748	2.106	0.0270	11
SPI	0.948	1.117	0.0007	12

285 The results presented in **Table 3** demonstrate that temperature (weight = 0.1784), distance from rivers (weight = 0.1112), NDVI (weight = 0.1089), and distance from roads (weight = 0.1065) are the parameters that have a significant impact on the formation of wildfire events within the study area.

Table 3 Assessment of multicollinearity and variable importance to wildfire influencing factors.

Factors	Wildfire			
	Tolerance	VIF	Variable importance	Rank
Temperature	0.643	1.555	0.1784	1

Distance from rivers	0.697	1.435	0.1112	2
NDVI	0.835	1.198	0.1089	3
Distance from roads	0.472	2.118	0.1065	4
Slope	0.512	1.954	0.0953	5
Rainfall in dry season	0.384	2.603	0.0739	6
LULC	0.737	1.356	0.0613	7
Profile Curvature	0.786	1.273	0.0538	8
Elevation	0.524	1.909	0.0500	9
Plan Curvature	0.715	1.398	0.0481	10
Aspect	0.513	1.948	0.0473	11
Lithology	0.551	1.816	0.0420	12
GeoHydrology	0.636	1.572	0.0233	13

4.2 Flood susceptibility map and model validation

For flood susceptibility models, the ROC curve analysis on the training dataset signifies that the CART model has the highest value of AUC (0.934), and the RF model has a lower AUC (0.921). The ROC curve analysis on the validation dataset reveals that the AUC value of the RF model (0.882) is higher than that of the CART model (0.845). This result demonstrates that the RF model has the best predictive performance for flood susceptibility mapping (**Figure 4**).

Since the RF shows good predictive performance, it is selected to generate the flood susceptibility map for the research area with the training dataset. The flood susceptibility map delineates the different geographical zones with increasing levels of susceptibility to flood events. We use the quantile method for classifying the susceptibility values with low (0-40%), moderate (40-70), high (70-90%), and very high (90-100%) classes and set the green-blue-yellow color scheme for flood susceptibility (**Figure 5**). The high and very high susceptibility areas are along the main river and the coastal zone, consistent with the flood inventory shown in **Figure 3**.
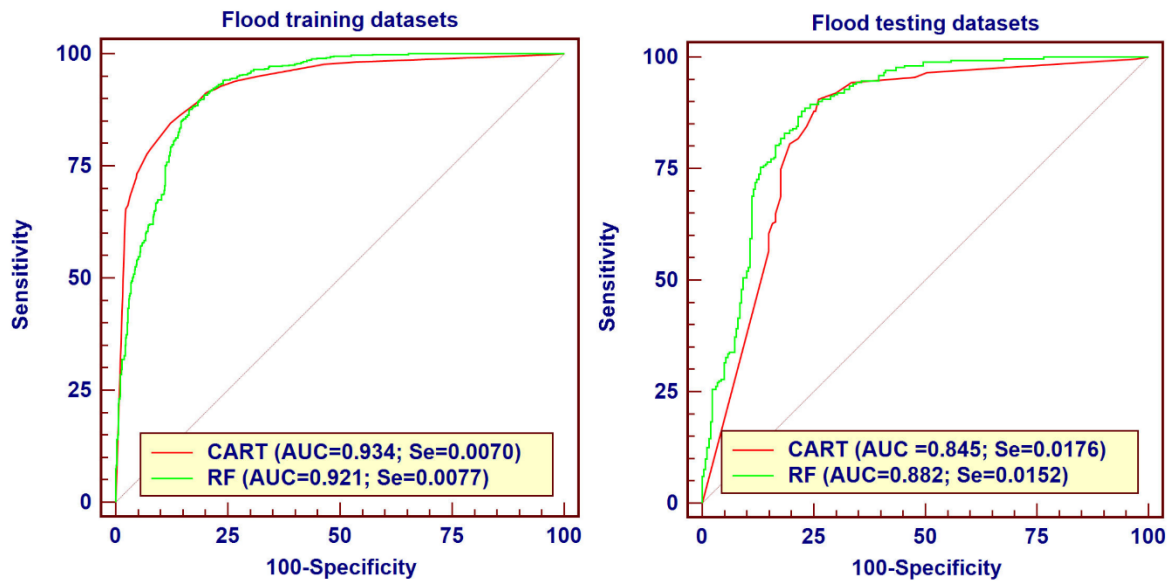
Figure 4. ROC curve and AUC analysis result from flood susceptibility modelling with training and validation datasets

(Note: Se stands for standard error)
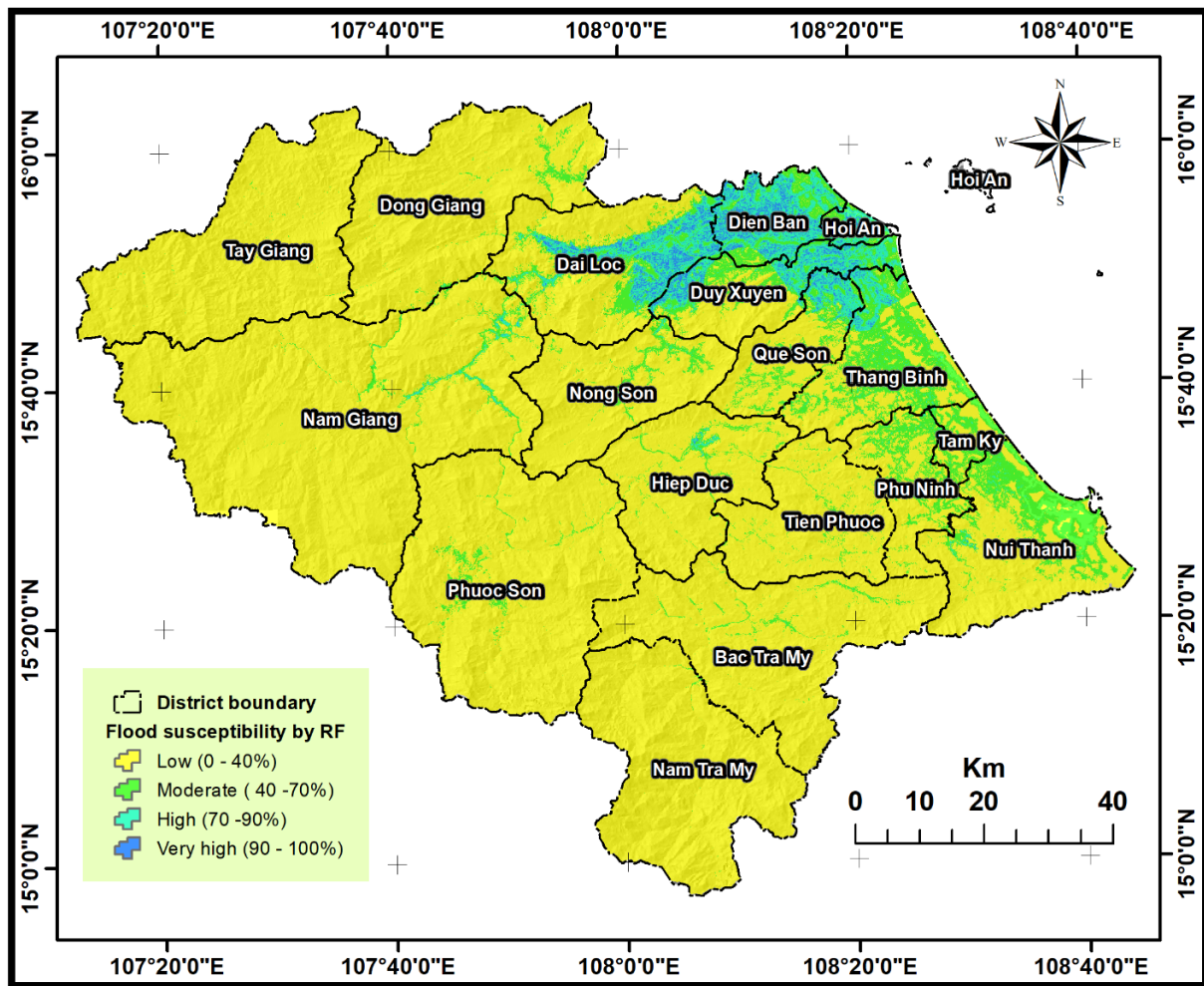
Figure 5. The flood susceptibility map derived using the RF model for Quang Nam province.

4.3 Wildfire susceptibility map and model validation

The ROC curve analysis on the training dataset for wildfire susceptibility models denotes that both the CART and RF models have the same AUC value (0.905). In contrast, the ROC curve analysis on the validation dataset reveals that the AUC value of the CART model (0.846) is lower than that of the RF model (0.884). This result reflects that the RF model is the best forecast model for wildfire susceptibility mapping (**Figure 6**).

Given the satisfactory predictive performance shown by the RF model, it has been chosen as the preferred method for generating fire susceptibility maps for the study area using the provided training dataset. The wildfire susceptibility map demarcates the diverse levels of susceptibility to fire occurrences. The same quantile approach is used to categorize susceptibility values. A green-yellow-red color scheme represents wildfire susceptibility (**Figure 7**). The areas highly prone

315 to wildfire hazards are in the middle highland, not the high mountainous or lowland areas, and agree with the wildfire distribution mapped in **Figure 3**.
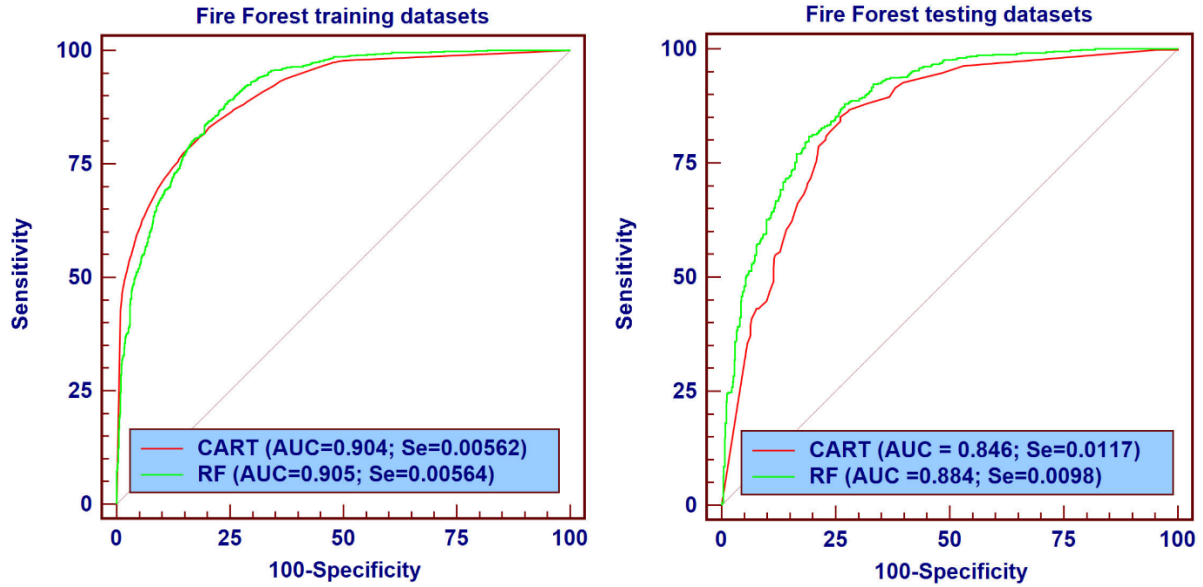
Figure 6. ROC curve and AUC analysis result from wildfire susceptibility modeling with training and testing datasets (Note: Se stands for standard error)

320
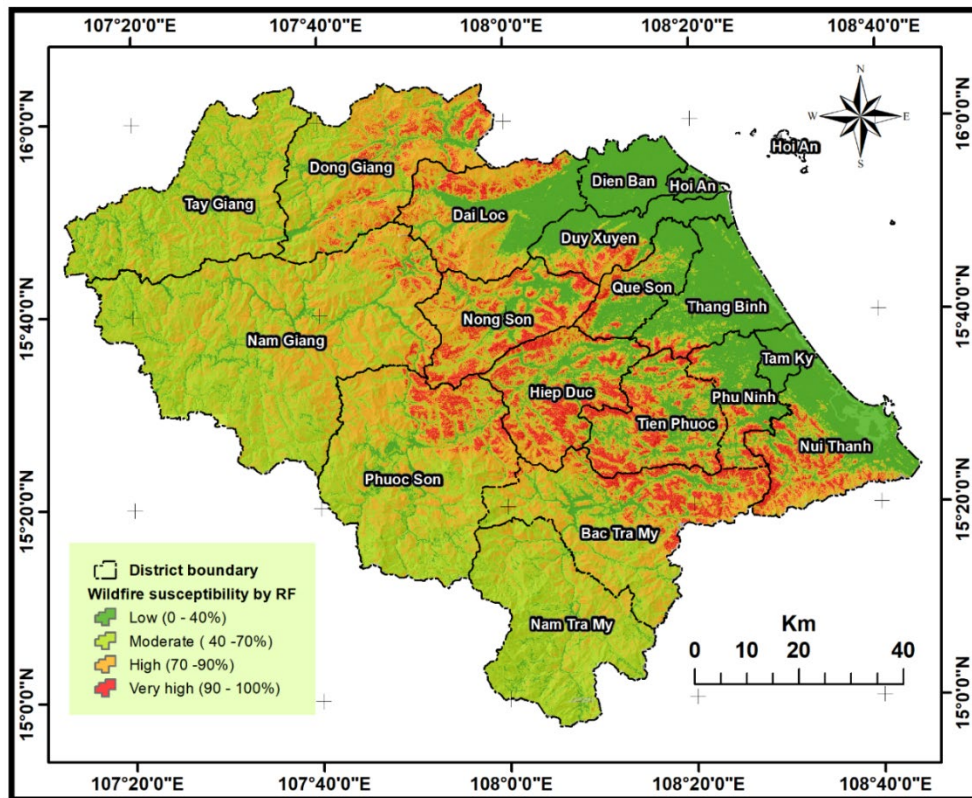
Figure 7. The wildfire susceptibility map was derived using the RF model for Quang Nam province.

4.4 Multi-hazard susceptibility and exposure mapping

The susceptibility map for hazard co-occurrence for Quang Nam province was generated by examining the spatial interplay between wildfire and floods. The map depicts a matrix-based classification that enables the definition of new susceptibility
325 classes (low, moderate, high, very high) of combined hazards and provides a unique multi-hazard profile for each location (**Figure 8**). In the matrix, not all combinations of hazards are represented, as there is no area with high susceptibility to floods and high susceptibility to wildfires. Combining the multi-hazards through a matrix gives a good visual overview of multi-hazards for the large scale of the whole province. The multi-hazard susceptibility map shows that the areas with very high wildfire susceptibility have low flood susceptibility and *vice versa*. The lowland coastal area is characterized by
330 moderate to very high flood hazards but limited fire hazards (categories 2, 3, 4). The mid-altitude slopes are categorized by low flood but high to very high fire hazards (categories 9-10, 13), except for possible floods along the main valleys, and the upland slopes are associated with moderate to low levels of the two hazards (categories 1, 2, 5).
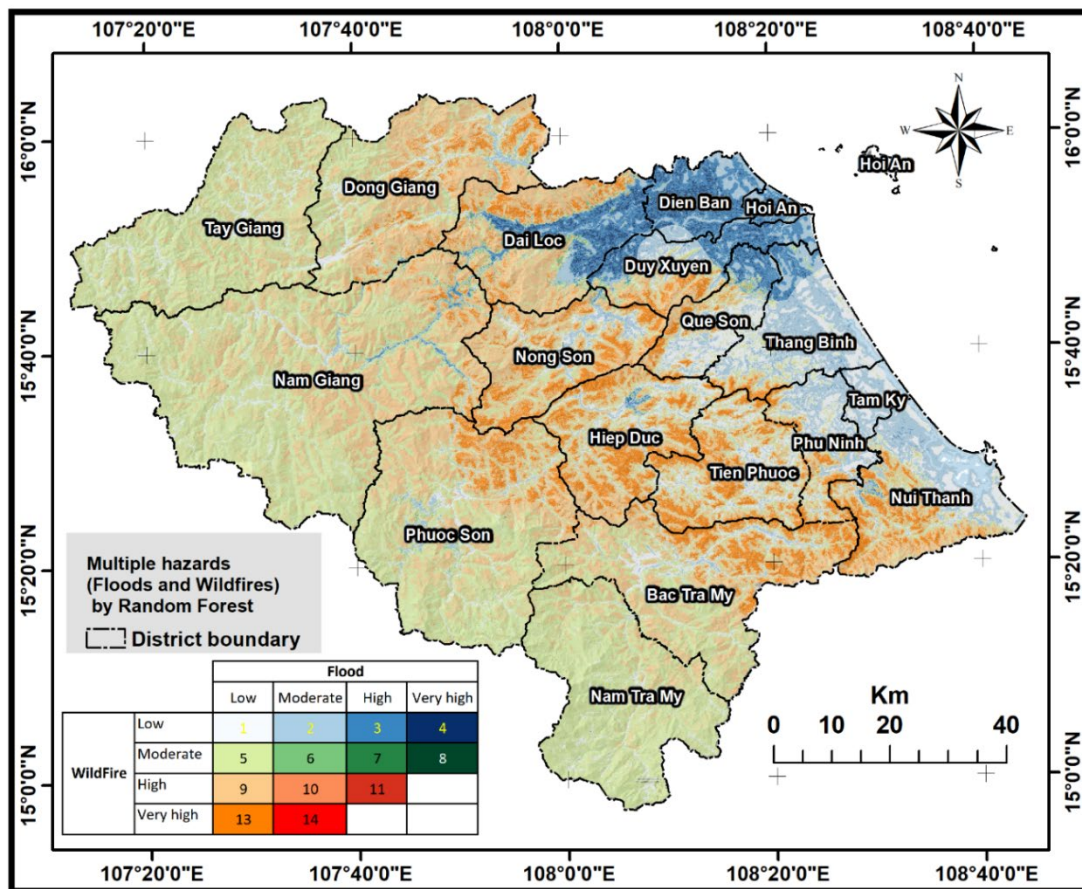
Figure 8. Integrated multi-hazard susceptibility classification combining flood and wildfire using random forest for Quang Nam province.

Our analysis examines the optimal sequence for integrating the two hazards, followed by assessing the exposure of buildings. The matrix of the number of buildings and area affected by each hazard level is converted into the percentage of total buildings in each cell of multi-hazard levels. We can compare the two in **Table 4**. It is highlighted that the proportion of buildings in the very high flood-low fire susceptibility category is much larger than the area of this category. In contrast, the proportion of buildings in category 13 (low flood - very high fire susceptibility) is much smaller than the area fraction. This highlights that measures to limit the impact on buildings (and so on people) to limit flood are much more important than for fire.

Table 4 Statistics of the percentage of buildings affected and the percentage of area represented in each cell by flood and wildfire hazard in Quang Nam province.

Buildings affected (%)		Flood			
		Low	Moderate	High	Very high
WildFire	Low	16.375	33.159	32.894	8.155

	Moderate	6.554	0.549	0.077	0.004
	High	2.037	0.033	0.001	
	Very high	0.162	0		

Area affected (%)		Flood			
		Low	Moderate	High	Very high
WildFire	Low	9.605	8.353	3.920	1.010
	Moderate	38.587	0.559	0.021	0.000
	High	29.966	0.118	0.000	
	Very high	7.859	0.002		

5 Discussion

Assessing susceptibility and exposure to several spatially co-occurring hazards is crucial and multifaceted in disaster management and community resilience (Menoni et al., 2012). In this study, floods and wildfires are examples of two hazards with different spatial patterns but quite similar spatial extent and frequency: assessment of the combined exposure to both hazards highlights that they have a very different impact on build-up infrastructure. Additional hazards, such as landslides or droughts, should be added to the scheme, with a multi-dimension hazard matrix/profiling of each zone. This would help define the hazard profile for each zone and identify which areas are indeed affected by multiple and maybe combining hazards (Yousefi et al., 2020).

ML models have been extensively used in diverse hazard evaluations, such as floods, landslides, and wildfire susceptibility (Bui et al., 2022; Ha et al., 2022; Pourtaghi et al., 2016). These techniques are advantageous in evaluating the efficacy of different models under comparable circumstances, considering similar influencing elements. This approach ensures a fair and unbiased determination of the most appropriate model for addressing a specific danger within a particular location. The modeling and mapping of multi-hazard susceptibility often rely on a system of multifaceted and multi-scaled natural factors, encompassing topography, geo-hydrology, environment, and hydro-meteorology conditions within the research area (Tavakkoli Piralilou et al., 2022).

Our research analyzed the combined exposure of buildings to flood and wildfire hazards in Quang Nam province, Vietnam. Utilizing ML models (CART and RF) to assess the susceptibility of multiple hazards, we can show that the RF model exhibited comparable levels of accuracy for both flood and wildfire hazards. Additionally, both models demonstrated good performance for flood and wildfire susceptibility maps, aligning with earlier research findings (Hasanzadeh Nafari et al., 2016; Nachappa et al., 2020). The accuracy of a model is dependent on the selection of the influencing elements used in mapping natural hazard susceptibility (Pourtaghi et al., 2016). This study carefully checked multicollinearity for influential factors and variable importance was measured to find the most suitable factors for the modeling input. In addition, the

selection of the non-hazard points is also thoroughly carried out with the specific standards, contributing to better modeling performance.

The integration of the susceptibility maps of flood and wildfire hazards into a multi-hazards susceptibility matrix highlights that flood and wildfire events threaten different areas and proportions of the entire Quang Nam province. The multi-hazard map is built upon a susceptibility class matrix for flood and wildfire events instead of a simple summation of both susceptibility maps. Indeed, the matrix enables the identification of regions with different combinations of hazard susceptibility for floods and wildfires. The exposure maps generated by combining the susceptibility map with the built environment data exhibit the total exposed housing for different susceptibility levels of each hazard and muti-hazards. Creating a multi-hazard exposure map that effectively delineates regions susceptible to floods and wildfires via implementing a matrix-based approach and combining the map with built environment data to assess the exposure elements of the hazards has not previously been attempted by other researchers. The combination with exposure highlights that different districts have to deal with different combinations of hazard susceptibility and that exposure to fire is much lower than flood hazards despite the broad spatial distribution of the wildfire susceptibility. This combination is an important step towards an integrated risk assessment of spatially co-occurring hazards; however, the contrasted vulnerability of buildings relative to different hazards, taking into account the specific attributes of the building, is also crucial in controlling the potential damage (Šakić Trogrlić et al., 2024). Such hazard-specific vulnerability functions for different building types still need to be constrained for the study area before a fully quantitative risk assessment can be completed.

Verifying multi-hazard exposure assessments is essential for ensuring the accuracy and reliability of the analysis, as well as for facilitating effective risk management strategies (Skilodimou et al., 2019). The multi-hazard exposure can be verified by analyzing historical damage data or examining the observed damage to vulnerable assets such as buildings, infrastructure, and natural resources (Khan et al., 2020). The 2020 flood and storm events caused 46 deaths, more than 117,000 properties have been flooded and damaged, and widespread damage to farmland, roads, irrigation works, and other infrastructure (Vdma, 2020). In addition, according to statistics from the Forest Protection Department of Quang Nam province, over the past five years in Quang Nam, there have been 136 forest fires causing damage to more than 618 hectares of various types of forests (available at https://chicuckiemlam.snnptnt.quangnam.gov.vn/). These available statistics confirmed the larger exposure of buildings to flood than to wildfire, as highlighted in Table 4. However the lack of damage statistics per hazard type at a fine spatial resolution prevent the comparison of our multi-hazard exposure map with actual recorded damage.

Considering the spatial occurrence of hazards and the associated exposure to build-up environment enables highlighting which areas and which proportion of buildings are exposed to one specific hazard or both, which can already be relevant for risk management. To consider temporal relationships between hazards (i.e., fire during the dry season inducing flood in the next rain season) or non-local dynamic interactions (i.e., wildfire in upper catchment increasing flood occurrence downstream) would require more process-oriented hazard modeling at a more local scale. A more complex physically-based model, typically at the scale of a smaller river catchment, would be required to investigate how the occurrence of one hazard influences the probability of occurrence of another hazard later in time and/or in the same or nearby location (Jenkins et al.,

2023). Another significant limitation of this research is the absence of consideration for stakeholder engagement and feedback while developing and applying the multi-hazard exposure estimation model. Interaction with stakeholders in charge of risk management would help to identify further the challenges posed by exposure to multi-hazard, validate the modeling approach proposed in this research, and specify how the result of such model can best contribute to strengthening the

405   effectiveness of risk management strategies.

6 Conclusion

This study produced an integrated approach to assess the climate hazards of floods and wildfires. We explored the assessment of several spatially co-occuring hazards and associated building exposure through an ML modeling approach. Through investigation of the flood and wildfire hazards and the impacts of those hazards on the built environment, our

410   modeling approach consisted of collating a database of recorded hazard footprints, topography, climate, geology, and environment data to input into our model and developing ML models for hazards modeling and coding in GEE to produce credible susceptibility and exposure maps. The susceptibility evaluation incorporated a matrix that combined hazards associated with flooding and wildfires. The integration of built environment data with the multi-hazard map facilitated an assessment of the potential exposure to multi-hazards across the region. Going forward, the potential for digitally-generated,

415   multi-hazard, and exposure maps for other climate-related hazards, such as landslides or drought, would further aid the identification of regions susceptible to these disasters and facilitate a rapid assessment of the consequences of these events. This research has demonstrated that effective maps can be developed using readily available and accessible data and ML tools that should help inform communities and regulatory authorities in Vietnam and beyond about the likelihood of risk and impacts from climate-related hazards. This research has the potential to provide clear information that will inform the

420   development and implementation of long-term risk reduction and adaptation strategies. Our findings suggest that ML models such as CART and RF could be used to analyze multi-hazard exposure for various geographical areas particularly susceptible to recurring incidents of wildfire and floods. Our data has shown that these tools can model risk and exposure effectively. However, the applied methods in this study did not account for the changes in the physical system induced by either floods or wildfires. The multi-hazard exposure maps for Quang Nam province offer valuable insights to planners,

425   disaster management specialists, and regional authorities, enabling them to adopt more effective management strategies for minimizing the many hazards present in the area. This approach may also facilitate the development of comprehensive strategies that address areas of high exposure to both hazards rather than focusing on individual hazards.

Acknowledgments

430   We sincerely thank the British Council for funding the UK/Viet Nam Season 2023 project "Evaluation of risks from multi-natural hazards and enhancing community adaptation capacities for Vietnam". We also acknowledge additional financial support from the VLIR-UOS TEAM Project (VN2022TEA533A105), "GEOdata infrastructures and citizen SCIences to support REsilient development of rural communities in Quang Nam province (GEOSCIRE)", for completing the publication of this manuscript.

435   **Author contributions**

CL, MK, GF, and LY conceived and designed the study. CL organized the study. QDB, HH, HCD, HHT, and DQN collected and processed the hazard inventories and input data. QDB analyzed the results and prepared the figures with the help of CL and MK. CL and HH wrote the manuscript. MK, GF, and LY edited the manuscript. All authors discussed the results and contributed with paper revisions.

440   **Competing interests**

The contact author has declared that none of the authors has any competing interests.

References

Abedi Gheshlaghi, H., Feizizadeh, B., Blaschke, T., Lakes, T., and Tajbar, S.: Forest fire susceptibility modeling using hybrid approaches, Transactions in GIS, 25, 311-333, https://doi.org/10.1111/tgis.12688, 2021.

445   Abram, N. J., Henley, B. J., Sen Gupta, A., Lippmann, T. J. R., Clarke, H., Dowdy, A. J., Sharples, J. J., Nolan, R. H., Zhang, T., Wooster, M. J., Wurtzel, J. B., Meissner, K. J., Pitman, A. J., Ukkola, A. M., Murphy, B. P., Tapper, N. J., and Boer, M. M.: Connections of climate change and variability to large and extreme forest fires in southeast Australia, Communications Earth & Environment, 2, 10.1038/s43247-020-00065-8, 2021.

Ahmadlou, M., Ebrahimian Ghajari, Y., and Karimi, M.: Enhanced classification and regression tree (CART) by genetic

450   algorithm (GA) and grid search (GS) for flood susceptibility mapping and assessment, Geocarto International, 37, 13638-13657, 10.1080/10106049.2022.2082550, 2022.

Ahmadlou, M., Karimi, M., Alizadeh, S., Shirzadi, A., Parvinnejhad, D., Shahabi, H., and Panahi, M.: Flood susceptibility assessment using integration of adaptive network-based fuzzy inference system (ANFIS) and biogeography-based optimization (BBO) and BAT algorithms (BA), Geocarto International, 34, 1252-1272, 10.1080/10106049.2018.1474276,

455   2018.

Ansori, S.: The Politics of Forest Fires in Southeast Asia, Contemporary Southeast Asia, 43, 179-202, 2021.

Arabameri, A., Pradhan, B., Rezaei, K., Yamani, M., Pourghasemi, H. R., and Lombardo, L.: Spatial modelling of gully erosion using evidential belief function, logistic regression, and a new ensemble of evidential belief function–logistic regression algorithm, Land Degradation & Development, 29, 4035-4049, 10.1002/ldr.3151, 2018.

460   Askar, R., Bragança, L., and Gervásio, H.: Adaptability of Buildings: A Critical Review on the Concept Evolution, Applied Sciences, 11, 10.3390/app11104483, 2021.

Balica, S. F., Dinh, Q., and Popescu, I.: Chapter 5 - Vulnerability and Exposure in Developed and Developing Countries: Large-Scale Assessments, in: Hydro-Meteorological Hazards, Risks and Disasters, edited by: Baldassarre, J. F. S. P. D., Elsevier, Boston, 125-162, http://dx.doi.org/10.1016/B978-0-12-394846-5.00005-9, 2015.

465 Bangalore, M., Smith, A., and Veldkamp, T.: Exposure to Floods, Climate Change, and Poverty in Vietnam, Economics of Disasters and Climate Change, 3, 79-99, 10.1007/s41885-018-0035-4, 2018.

Bountzouklis, C., Fox, D. M., and Di Bernardino, E.: Environmental factors affecting wildfire-burned areas in southeastern France, 1970–2019, Natural Hazards and Earth System Sciences, 22, 1181-1200, 10.5194/nhess-22-1181-2022, 2022.

Breiman, L.: Random Forests, Machine Learning, 45, 5-32, https://doi.org/10.1023/a:1010933404324, 2001.

470 Breiman, L., Friedman, J., Olshen, R., and Stone, C.: Classification and regression trees, Classification and regression trees, CRC press1984.

Bui, Q. D., Luu, C., Mai, S. H., Ha, H. T., Ta, H. T., and Pham, B. T.: Flood risk mapping and analysis using an integrated framework of machine learning models and analytic hierarchy process, Risk Anal, 10.1111/risa.14018, 2022.

Bui, Q. D., Ha, H., Khuc, D. T., Nguyen, D. Q., von Meding, J., Nguyen, L. P., and Luu, C.: Landslide susceptibility
475 prediction mapping with advanced ensemble models: Son La province, Vietnam, Natural Hazards, 116, 2283-2309, 10.1007/s11069-022-05764-3, 2023.

Carreño, M. L., Cardona, O. D., and Barbat, A. H.: A disaster risk management performance index, Natural Hazards, 41, 1-20, https://doi.org/10.1007/s11069-006-9008-y, 2007.

Carter, J. V., Pan, J., Rai, S. N., and Galandiuk, S.: ROC-ing along: Evaluation and interpretation of receiver operating
480 characteristic curves, Surgery, 159, 1638-1645, https://doi.org/10.1016/j.surg.2015.12.029, 2016.

Chau, V. N., Cassells, S., and Holland, J.: Economic impact upon agricultural production from extreme flood events in Quang Nam, central Vietnam, Natural Hazards, 75, 1747-1765, https://doi.org/10.1007/s11069-014-1395-x, 2014.

Chen, W., Xie, X., Peng, J., Shahabi, H., Hong, H., Bui, D. T., Duan, Z., Li, S., and Zhu, A. X.: GIS-based landslide susceptibility evaluation using a novel hybrid integration approach of bivariate statistical based random forest method,
485 CATENA, 164, 135-149, https://doi.org/10.1016/j.catena.2018.01.012, 2018.

De Angeli, S., Malamud, B. D., Rossi, L., Taylor, F. E., Trasforini, E., and Rudari, R.: A multi-hazard framework for spatial-temporal impact analysis, International Journal of Disaster Risk Reduction, 73, 102829, 10.1016/j.ijdrr.2022.102829, 2022.

Dottori, F., Martina, M. L. V., and Figueiredo, R.: A methodology for flood susceptibility and vulnerability analysis in complex flood scenarios, Journal of Flood Risk Management, 11, S632-S645, https://doi.org/10.1111/jfr3.12234, 2018.

490 Du, T. L. T., Bui, D. D., Nguyen, M. D., and Lee, H.: Satellite-Based, Multi-Indices for Evaluation of Agricultural Droughts in a Highly Dynamic Tropical Catchment, Central Vietnam, Water, 10, 10.3390/w10050659, 2018.

Eisenbies, M. H., Aust, W. M., Burger, J. A., and Adams, M. B.: Forest operations, extreme flooding events, and considerations for hydrologic modeling in the Appalachians—A review, Forest Ecology and Management, 242, 77-98, 10.1016/j.foreco.2007.01.051, 2007.

495 Fox, E. W., Hill, R. A., Leibowitz, S. G., Olsen, A. R., Thornbrugh, D. J., and Weber, M. H.: Assessing the accuracy and stability of variable selection methods for random forest modeling in ecology, Environmental monitoring and assessment, 189, 1-20, 10.1007/s10661-017-6025-0, 2017.

Gan, C. C. R., Oktari, R. S., Nguyen, H. X., Yuan, L., Yu, X., Kc, A., Hanh, T. T. T., Phung, D. T., Dwirahmadi, F., Liu, T., Musumari, P. M., Kayano, R., and Chu, C.: A scoping review of climate-related disasters in China, Indonesia and Vietnam:
500 Disasters, health impacts, vulnerable populations and adaptation measures, International Journal of Disaster Risk Reduction, 66, 102608, https://doi.org/10.1016/j.ijdrr.2021.102608, 2021.

Genuer, R., Poggi, J.-M., and Tuleau-Malot, C.: Variable selection using random forests, Pattern Recognition Letters, 31, 2225-2236, https://doi.org/10.1016/j.patrec.2010.03.014, 2010.

Giglio, L., Csiszar, I., Restás, Á., Morisette, J. T., Schroeder, W., Morton, D., and Justice, C. O.: Active fire detection and
505 characterization with the advanced spaceborne thermal emission and reflection radiometer (ASTER), Remote Sensing of Environment, 112, 3055-3063, 10.1016/j.rse.2008.03.003, 2008.

Gonzalez-Arqueros, M. L., Mendoza, M. E., Bocco, G., and Solis Castillo, B.: Flood susceptibility in rural settlements in remote zones: The case of a mountainous basin in the Sierra-Costa region of Michoacan, Mexico, Journal of environmental management, 223, 685-693, https://doi.org/10.1016/j.jenvman.2018.06.075, 2018.

510 Ha, H., Bui, Q. D., Nguyen, H. D., Pham, B. T., Lai, T. D., and Luu, C.: A practical approach to flood hazard, vulnerability, and risk assessing and mapping for Quang Binh province, Vietnam, Environment, Development and Sustainability, 25, 1101-1130, 10.1007/s10668-021-02041-4, 2023.

Ha, H., Bui, Q. D., Khuc, T. D., Tran, D. T., Pham, B. T., Mai, S. H., Nguyen, L. P., and Luu, C.: A machine learning approach in spatial predicting of landslides and flash flood susceptible zones for a road network, Modeling Earth Systems

515 and Environment, 10.1007/s40808-022-01384-9, 2022.

Hasanzadeh Nafari, R., Ngo, T., and Mendis, P.: An Assessment of the Effectiveness of Tree-Based Models for Multi-Variate Flood Damage Assessment in Australia, Water, 8, 282, https://doi.org/10.3390/w8070282, 2016.

Hosseini, M. and Lim, S.: Gene expression programming and data mining methods for bushfire susceptibility mapping in New South Wales, Australia, Natural Hazards, 113, 1349-1365, 10.1007/s11069-022-05350-7, 2022.

520 IPCC: Climate Change 2022: Impacts, Adaptation and Vulnerability. Working Group II Contribution to the Sixth Assessment Report of the Intergovernmental Panel on Climate Change, Cambridge University Press, 2022.

Javidan, N., Kavian, A., Pourghasemi, H. R., Conoscenti, C., Jafarian, Z., and Rodrigo-Comino, J.: Evaluation of multi-hazard map produced using MaxEnt machine learning technique, Scientific reports, 11, 6496, 10.1038/s41598-021-85862-7, 2021.

525 Jenkins, L. T., Creed, M. J., Tarbali, K., Muthusamy, M., Trogrlić, R. Š., Phillips, J. C., Watson, C. S., Sinclair, H. D., Galasso, C., and McCloskey, J.: Physics-based simulations of multiple natural hazards for risk-sensitive planning and decision making in expanding urban regions, International Journal of Disaster Risk Reduction, 84, 10.1016/j.ijdrr.2022.103338, 2023.

Kalantar, B., Ueda, N., Idrees, M. O., Janizadeh, S., Ahmadi, K., and Shabani, F.: Forest fire susceptibility prediction based

530 on machine learning models with resampling algorithms on remote sensing data, Remote Sensing, 12, 3682, 10.3390/rs12223682, 2020.

Khan, A., Gupta, S., and Gupta, S. K.: Multi-hazard disaster studies: Monitoring, detection, recovery, and management, based on emerging technologies and optimal techniques, International Journal of Disaster Risk Reduction, 47, 101642, https://doi.org/10.1016/j.ijdrr.2020.101642, 2020.

535 Khatakho, R., Gautam, D., Aryal, K. R., Pandey, V. P., Rupakhety, R., Lamichhane, S., Liu, Y.-C., Abdouli, K., Talchabhadel, R., and Thapa, B. R.: Multi-hazard risk assessment of Kathmandu Valley, Nepal, Sustainability, 13, 5369, 10.3390/su13105369, 2021.

Kim, J.-C., Lee, S., Jung, H.-S., and Lee, S.: Landslide susceptibility mapping using random forest and boosted tree models in Pyeong-Chang, Korea, Geocarto International, 1-16, https://doi.org/10.1080/10106049.2017.1323964, 2017.

540 Lee, J., Perera, D., Glickman, T., and Taing, L.: Water-related disasters and their health impacts: A global review, Progress in Disaster Science, 8, 100123, https://doi.org/10.1016/j.pdisas.2020.100123, 2020.

Luu, C., Bui, Q. D., and von Meding, J.: Mapping direct flood impacts from a 2020 extreme flood event in Central Vietnam using spatial analysis techniques, International Journal of Disaster Resilience in the Built Environment, 14, 85-99, 10.1108/ijdrbe-07-2021-0070, 2021.

545 Luu, C., Von Meding, J., and Kanjanabootra, S.: Assessing flood hazard using flood marks and analytic hierarchy process approach: a case study for the 2013 flood event in Quang Nam, Vietnam, Natural Hazards, 90, 1031-1050, https://doi.org/10.1007/s11069-017-3083-0, 2018.

Ma, Y., Ma, B., Jiao, H., Zhang, Y., Xin, J., and Yu, Z.: An analysis of the effects of weather and air pollution on tropospheric ozone using a generalized additive model in Western China: Lanzhou, Gansu, Atmospheric Environment, 224,

550 117342, https://doi.org/10.1016/j.atmosenv.2020.117342, 2020.

Mai Sy, H., Luu, C., Bui, Q. D., Ha, H., and Nguyen, D. Q.: Urban flood risk assessment using Sentinel-1 on the google earth engine: A case study in Thai Nguyen city, Vietnam, Remote Sensing Applications: Society and Environment, 31, 10.1016/j.rsase.2023.100987, 2023.

Menoni, S., Molinari, D., Parker, D., Ballio, F., and Tapsell, S.: Assessing multifaceted vulnerability and resilience in order

555 to design risk-mitigation strategies, Natural hazards, 64, 2057-2082, 10.1007/s11069-012-0134-4, 2012.

Miao, F., Zhao, F., Wu, Y., Li, L., and Török, Á.: Landslide susceptibility mapping in Three Gorges Reservoir area based on GIS and boosting decision tree model, Stochastic Environmental Research and Risk Assessment, 1-21, 10.1007/s00477-023-02394-4, 2023.

Mueller, J. M., Lima, R. E., Springer, A. E., and Schiefer, E.: Using matching methods to estimate impacts of wildfire and postwildfire flooding on house prices, Water Resources Research, 54, 6189-6201, 10.1029/2017WR022195, 2018.

Nachappa, T., Ghorbanzadeh, O., Gholamnia, K., and Blaschke, T.: Multi-Hazard Exposure Mapping Using Machine Learning for the State of Salzburg, Austria, Remote Sensing, 12, 10.3390/rs12172757, 2020.

Naghibi, S. A., Pourghasemi, H. R., and Dixon, B.: GIS-based groundwater potential mapping using boosted regression tree, classification and regression tree, and random forest machine learning models in Iran, Environmental monitoring and assessment, 188, 1-27, 10.1007/s10661-015-5049-6, 2016.

Nguyen, T. V., Allen, K. J., Le, N. C., Truong, C. Q., Tenzin, K., and Baker, P. J.: Human-Driven Fire Regime Change in the Seasonal Tropical Forests of Central Vietnam, Geophysical Research Letters, 50, 10.1029/2022gl100687, 2023.

Papaioannou, G., Alamanos, A., and Maris, F.: Evaluating Post-Fire Erosion and Flood Protection Techniques: A Narrative Review of Applications, GeoHazards, 4, 380-405, 10.3390/geohazards4040022, 2023.

Pham, B. T., Luu, C., Phong, T. V., Nguyen, H. D., Le, H. V., Tran, T. Q., Ta, H. T., and Prakash, I.: Flood risk assessment using hybrid artificial intelligence models integrated with multi-criteria decision analysis in Quang Nam Province, Vietnam, Journal of Hydrology, 592, https://doi.org/10.1016/j.jhydrol.2020.125815, 2021.

Piao, Y., Lee, D., Park, S., Kim, H. G., and Jin, Y.: Multi-hazard mapping of droughts and forest fires using a multi-layer hazards approach with machine learning algorithms, Geomatics, Natural Hazards and Risk, 13, 2649-2673, 10.1080/19475705.2022.2128440, 2022.

Pourghasemi, H. R., Pouyan, S., Bordbar, M., Golkar, F., and Clague, J. J.: Flood, landslides, forest fire, and earthquake susceptibility maps using machine learning techniques and their combination, Natural Hazards, 116, 3797-3816, 10.1007/s11069-023-05836-y, 2023.

Pourghasemi, H. R., Kariminejad, N., Amiri, M., Edalat, M., Zarafshar, M., Blaschke, T., and Cerda, A.: Assessing and mapping multi-hazard risk susceptibility using a machine learning technique, Scientific reports, 10, 3203, 10.1038/s41598-020-60191-3, 2020.

Pourtaghi, Z. S., Pourghasemi, H. R., Aretano, R., and Semeraro, T.: Investigation of general indicators influencing on forest fire and its susceptibility modeling using different data mining techniques, Ecological Indicators, 64, 72-84, 10.1016/j.ecolind.2015.12.030, 2016.

Quang Nam Statistical Office, Dinh, V. H. (Ed.): Quang Nam statistical Yearbook 2019, Statistical Publishing House, Vietnam2019.

Rentschler, J., Salhab, M., and Jafino, B. A.: Flood exposure and poverty in 188 countries, Nat Commun, 13, 3527, 10.1038/s41467-022-30727-4, 2022.

Rusk, J., Maharjan, A., Tiwari, P., Chen, T.-H. K., Shneiderman, S., Turin, M., and Seto, K. C.: Multi-hazard susceptibility and exposure assessment of the Hindu Kush Himalaya, Science of The Total Environment, 804, 150039, https://doi.org/10.1016/j.scitotenv.2021.150039, 2022.

Šakić Trogrlić, R., Thompson, H. E., Menteşe, E. Y., Hussain, E., Gill, J. C., Taylor, F. E., Mwangi, E., Öner, E., Bukachi, V. G., and Malamud, B. D.: Multi-Hazard Interrelationships and Risk Scenarios in Urban Areas: A Case of Nairobi and Istanbul, Earth's Future, 12, 10.1029/2023ef004413, 2024.

Schneiderbauer, S. and Ehrlich, D.: Risk, hazard and people's vulnerability to natural hazards, A review of definitions, concepts and data. European Commission Joint Research Centre. EUR, 21410, 40, 2004.

Schratz, P., Muenchow, J., Iturritxa, E., Richter, J., and Brenning, A.: Hyperparameter tuning and performance assessment of statistical and machine-learning algorithms using spatial data, Ecological Modelling, 406, 109-120, 10.1016/j.ecolmodel.2019.06.002, 2019.

Sirko, W., Kashubin, S., Ritter, M., Annkah, A., Bouchareb, Y. S. E., Dauphin, Y., Keysers, D., Neumann, M., Cisse, M., and Quinn, J.: Continental-scale building detection from high resolution satellite imagery, arXiv preprint arXiv:2107.12283, 2021.

Skilodimou, H. D., Bathrellos, G. D., and Alexakis, D. E.: Flood hazard assessment mapping in burned and urban areas, Sustainability, 13, 4455, 10.3390/su13084455, 2021.

Skilodimou, H. D., Bathrellos, G. D., Chousianitis, K., Youssef, A. M., and Pradhan, B.: Multi-hazard assessment modeling via multi-criteria analysis and GIS: a case study, Environmental Earth Sciences, 78, 1-21, 10.1007/s12665-018-8003-4, 2019.

Tamiminia, H., Salehi, B., Mahdianpari, M., Quackenbush, L., Adeli, S., and Brisco, B.: Google Earth Engine for geo-big data applications: A meta-analysis and systematic review, ISPRS Journal of Photogrammetry and Remote Sensing, 164, 152-170, https://doi.org/10.1016/j.isprsjprs.2020.04.001, 2020.

Tang, R. and Zhang, X.: CART decision tree combined with Boruta feature selection for medical data classification, 2020 5th IEEE International Conference on Big Data Analytics (ICBDA), 80-84, 10.1109/ICBDA49040.2020.9101199,

Tavakkoli Piralilou, S., Einali, G., Ghorbanzadeh, O., Nachappa, T. G., Gholamnia, K., Blaschke, T., and Ghamisi, P.: A Google Earth Engine approach for wildfire susceptibility prediction fusion with remote sensing data of different spatial resolutions, Remote sensing, 14, 672, 10.3390/rs14030672, 2022.

Tedim, F., Xanthopoulos, G., and Leone, V.: Chapter 5 - Forest Fires in Europe: Facts and Challenges, in: Wildfire Hazards, Risks and Disasters, edited by: Shroder, J. F., and Paton, D., Elsevier, Oxford, 77-99, https://doi.org/10.1016/B978-0-12-410434-1.00005-1, 2015.

Trang, P. T., Andrew, M. E., Chu, T., and Enright, N. J.: Forest fire and its key drivers in the tropical forests of northern Vietnam, International Journal of Wildland Fire, 31, 213-229, 10.1071/wf21078, 2022.

Flash Update No. 4: Viet Nam Floods, Landslides and Storms (As of 28 October 2020): http://phongchongthientai.mard.gov.vn/en/Pages/flash-update-no-4-viet-nam-floods-landslides-and-storms-as-of-28-october-2020-.aspx?item=/en/Pages/flash-update-no-4-viet-nam-floods-landslides-and-storms-as-of-28-october-2020-.aspx, last access: 28 October 2020.

Velev, D. and Zlateva, P.: Challenges Of Artificial Intelligence Application For Disaster Risk Management, The International Archives of the Photogrammetry, Remote Sensing and Spatial Information Sciences, 48, 387-394, 10.5194/isprs-archives-XLVIII-M-1-2023-387-2023, 2023.

Wang, J., He, Z., and Weng, W.: A review of the research into the relations between hazards in multi-hazard risk analysis, Natural Hazards, 104, 2003-2026, 10.1007/s11069-020-04259-3, 2020.

Wing, O. E. J., Bates, P. D., Smith, A. M., Sampson, C. C., Johnson, K. A., Fargione, J., and Morefield, P.: Estimates of present and future flood risk in the conterminous United States, Environmental Research Letters, 13, 10.1088/1748-9326/aaac65, 2018.

Wu, W., Zhang, Q., Singh, V. P., Wang, G., Zhao, J., Shen, Z., and Sun, S.: A Data-Driven Model on Google Earth Engine for Landslide Susceptibility Assessment in the Hengduan Mountains, the Qinghai–Tibetan Plateau, Remote Sensing, 14, 4662, 10.3390/rs14184662, 2022.

Yousefi, S., Pourghasemi, H. R., Emami, S. N., Pouyan, S., Eskandari, S., and Tiefenbacher, J. P.: A machine learning framework for multi-hazards modeling and mapping in a mountainous area, Sci Rep, 10, 12144, 10.1038/s41598-020-69233-2, 2020.

Yu, G., Liu, T., McGuire, L. A., Wright, D. B., Hatchett, B. J., Miller, J. J., Berli, M., Giovando, J., Bartles, M., and Floyd, I. E.: Process-Based Quantification of the Role of Wildfire in Shaping Flood Frequency, Water Resources Research, 59, e2023WR035013, 10.1029/2023WR035013, 2023.

Zhou, Y., Liu, Y., Wu, W., and Li, N.: Integrated risk assessment of multi-hazards in China, Natural hazards, 78, 257-280, 10.1007/s11069-015-1713-y, 2015.